Ion-cyclotron instability in plasmas described by product-bi-kappa distributions

M. S. dos Santos, L. F. Ziebell, and R. Gaelzer

Citation: Physics of Plasmas **22**, 122107 (2015); doi: 10.1063/1.4936972
View online: http://dx.doi.org/10.1063/1.4936972
View Table of Contents: http://scitation.aip.org/content/aip/journal/pop/22/12?ver=pdfcov
Published by the AIP Publishing

Ion-cyclotron instability in plasmas described by product-bi-kappa distributions

M. S. dos Santos, L. F. Ziebell,[a] and R. Gaelzer[b]
Instituto de Física, Universidade Federal do Rio Grande do Sul, Caixa Postal 15051, CEP: 91501-970 Porto Alegre, RS, Brazil

(Received 26 October 2015; accepted 20 November 2015; published online 9 December 2015)

The dispersion relation for parallel propagating waves in the ion-cyclotron branch is investigated numerically by considering that the velocity distribution of the ion population is a function of type product-bi-kappa. We investigate the effects of the non-thermal features and of the anisotropy associated with this type of distribution on the ion-cyclotron instability, as well as the influence of different forms of the electron distribution, by considering Maxwellian distributions, bi-kappa distributions, and product-bi-kappa distributions. The cases of ions described by either Maxwellian or bi-kappa distributions are also considered, for comparison. The results of the numerical analysis show that the increase in the non-thermal character associated with the anisotropic kappa distributions for ions contributes to enhance the instability as compared to that obtained in the Maxwellian case, in magnitude and in wave number range, with more significant enhancement for the case of ion product-bi-kappa distributions than for the case of ion bi-kappa distributions. It is also shown that the ion-cyclotron instability is decreased if the electrons are described by product-bi-kappa distributions, while electrons described by bi-kappa distributions lead to growth rates which are very similar to those obtained considering a Maxwellian distribution for the electron population. © *2015 AIP Publishing LLC*. [http://dx.doi.org/10.1063/1.4936972]

I. INTRODUCTION

The instability which is known as ion-cyclotron instability (IC) may occur when the dispersion of velocities of the plasma particles along the direction perpendicular to the direction of the ambient magnetic field is larger than the velocity dispersion along parallel direction. This type of instability has attracted continued interest, particularly from the community interested in physical processes in space plasmas, since the observations consistently show the presence of anisotropic velocity distributions for particles under different space plasma conditions.[1–5] The ion-cyclotron instability is commonly described by considering anisotropic Maxwellian distributions, and it can be said that it is associated with the condition $T_{i\perp}/T_{i\|} > 1$, where i indicates the ion population and $T_\perp$, $T_\|$, respectively, represent the perpendicular and parallel temperatures.[6,7] However, observations have shown that plasma particles in space conditions frequently display non-thermal tails and anisotropies, which are not well described by Maxwellian distributions,[1–5] leading to the introduction of distributions with power-law tails, generally known as *kappa distributions*.[8–14] In fact, there is abundance of evidence of non-thermal features in velocity distributions of plasma particles in spatial environments, a situation which has fueled a growing interest in the study of space phenomena considering the presence of kappa distributions, as can be appreciated by the list of citations of a relatively recent and abrangent paper on the subject.[15]

Among the existing works, it is of particular interest for the present investigation to mention studies on low-frequency electromagnetic instabilities, related to the ion-cyclotron instability[16,17] or to the ion firehose instability,[18–20] which have been made considering kappa velocity distributions. These studies have most commonly assumed anisotropic kappa distributions which are known as *bi-kappa distributions* (BKs), characterized by a single kappa index and anisotropic parameters related to the temperature,[11,16,18–20] although some analyses can be found that have introduced the so-called *product-bi-kappa distributions* (PBK), which may feature anisotropic kappa indexes in addition to anisotropic temperature parameters.[17,21] However, PBK distributions are not yet widely found in studies of plasma instabilities, although it is already recognized that distributions of this type can be useful for the analysis of the limits for the occurrence of instabilities, mostly because of their greater flexibility for the description of highly anisotropic and non-thermal features, which are frequently found in the space plasma environment.[22]

In the present paper, we study the dispersion relation for the ion-cyclotron instability, considering that the velocity distributions of ions are PBK distributions, and considering that the electron distribution can be a PBK distribution, a BK distribution, or a Maxwellian distribution. The approach is similar to that which we used in a recent investigation about the ion firehose instability.[21] We obtain the general form of the dispersion relation and then discuss the numerical solution considering different situations. For comparison, we also present results obtained considering ions described by bi-Maxwellian distributions and by BK distributions. The organization of the paper is as follows: In Section II, we briefly describe the theoretical formulation and the dispersion relation for electromagnetic waves propagating parallel to the

[a]Electronic mail: luiz.ziebell@ufrgs.br
[b]Electronic mail: rudi.gaelzer@ufrgs.br

ambient magnetic field, considering the particular cases of plasma particles with PBK, BK, and bi-Maxwellian distribution functions. In Section III, we present and discuss results obtained by numerical solution of the dispersion relation, for several combinations of distribution functions. Final remarks and a discussion on future perspectives appear in Section IV.

II. THEORETICAL FORMULATION

The general dispersion relation for parallel propagation can be separated into two branches, one of them related to electrostatic waves and the other related to electromagnetic waves which are circularly polarized. For this branch of electromagnetic waves, there are two possibilities of sign ($s=\pm 1$), and it is easy to show that the dispersion relation can be written as follows:[21]

$$N_{\parallel}^2 = 1 + \frac{1}{2}\sum_{\beta}\frac{\omega_{p\beta}^2}{\omega^2}\frac{1}{n_{\beta 0}}J(s,1,0;f_{\beta 0}), \tag{1}$$

where J is an integral expression, which is dependent of the distribution function of the particles

$$J(n,m,h;f_{\beta 0}) \equiv \omega\int d^3v\,\frac{v_{\parallel}^h v_{\perp}^{2(m-1)} v_{\perp} L(f_{\beta 0})}{\omega - n\Omega_{\beta} - k_{\parallel}v_{\parallel}}, \tag{2}$$

and where L and $\mathcal{L}$ are differential operators

$$L = \left[\left(1-\frac{k_{\parallel}v_{\parallel}}{\omega}\right)\frac{\partial}{\partial v_{\perp}} + \frac{k_{\parallel}v_{\perp}}{\omega}\frac{\partial}{\partial v_{\parallel}}\right],$$
$$\mathcal{L} = v_{\parallel}\frac{\partial}{\partial v_{\perp}} - v_{\perp}\frac{\partial}{\partial v_{\parallel}},$$

with

$$\omega_{p\beta}^2 = \frac{4\pi n_{\beta 0} q_{\beta}^2}{m_{\beta}}, \quad \Omega_{\beta} = \frac{q_{\beta}B_0}{m_{\beta}c}, \quad N_{\parallel} = \frac{ck_{\parallel}}{\omega}.$$

Let us now discuss different forms of anisotropic velocity distributions $f_{\beta 0}$, and obtain the corresponding form of the integral expression $J(n, m, h; f_{\beta 0})$, which contributes to the dispersion relation (1).

Initially, we consider the case of plasma particles described by anisotropic kappa distributions characterized by anisotropic kappa indexes, also known as PBK distributions

$$f_{\beta,\kappa}(v_{\parallel},v_{\perp}) = \frac{n_{\beta 0}}{\pi^{3/2}\kappa_{\beta\perp}\kappa_{\beta\parallel}^{1/2}v_{\beta\perp}^2 v_{\beta\parallel}} \times \frac{\Gamma(\kappa_{\beta\perp})\Gamma(\kappa_{\beta\parallel})}{\Gamma(\kappa_{\beta\perp}-1)\Gamma(\kappa_{\beta\parallel}-1/2)} \times \left(1+\frac{v_{\parallel}^2}{\kappa_{\beta\parallel}v_{\beta\parallel}^2}\right)^{-\kappa_{\beta\parallel}}\left(1+\frac{v_{\perp}^2}{\kappa_{\beta\perp}v_{\beta\perp}^2}\right)^{-\kappa_{\beta\perp}}, \tag{3}$$

where

$$v_{\beta\parallel}^2 = \frac{2T_{\beta\parallel}}{m_{\beta}}, \quad v_{\beta\perp}^2 = \frac{2T_{\beta\perp}}{m_{\beta}}.$$

In order to avoid negative arguments in the Γ functions, the range of values of the κ indexes has to be restricted to $\kappa_{\parallel} > 0.5$ and $\kappa_{\perp} > 1.0$.

We can define effective parallel and perpendicular temperatures for particles with velocity distribution described by Equation (3), using energy units, as follows:

$$\begin{pmatrix}\frac{1}{2}\theta_{\beta\parallel}\\ \theta_{\beta\perp}\end{pmatrix} = \frac{m_{\beta}}{\pi^{1/2}\kappa_{\beta\perp}\kappa_{\beta\parallel}^{1/2}v_{\beta\perp}^2 v_{\beta\parallel}}\frac{\Gamma(\kappa_{\beta\perp})\Gamma(\kappa_{\beta\parallel})}{\Gamma(\kappa_{\beta\perp}-1)\Gamma(\kappa_{\beta\parallel}-1/2)} \times \int_{-\infty}^{\infty}dv_{\parallel}\left(1+\frac{v_{\parallel}^2}{\kappa_{\beta\parallel}v_{\beta\parallel}^2}\right)^{-\kappa_{\beta\parallel}} \times \int_{0}^{\infty}dv_{\perp}\,v_{\perp}\left(1+\frac{v_{\perp}^2}{\kappa_{\beta\perp}v_{\beta\perp}^2}\right)^{-\kappa_{\beta\perp}}\begin{pmatrix}v_{\parallel}^2\\ v_{\perp}^2\end{pmatrix}. \tag{4}$$

Upon evaluation of the integrals, it is easy to show that the ratio of effective temperatures is given by

$$\frac{\theta_{\beta\perp}}{\theta_{\beta\parallel}} = \frac{\kappa_{\beta\perp}(\kappa_{\beta\parallel}-3/2)}{\kappa_{\beta\parallel}(\kappa_{\beta\perp}-2)}\frac{T_{\beta\perp}}{T_{\beta\parallel}}. \tag{5}$$

In what follows, the quantities $\theta_{\beta\perp}$ and $\theta_{\beta\parallel}$ will be denominated "effective temperatures," while the quantities $T_{\beta\perp}$ and $T_{\beta\parallel}$ will be denominated "temperatures."

Using the distribution function given by Equation (3), the integral defined in Eq. (2) may be evaluated, and we obtain the following:[23]

$$J(s,1,0;f_{\beta 0}) = 2n_{\beta 0}\frac{\kappa_{\beta\perp}}{\kappa_{\beta\perp}-2}\times\left[-\frac{\kappa_{\beta\perp}-2}{\kappa_{\beta\perp}}+\frac{u_{\beta\perp}^2}{u_{\beta\parallel}^2}\frac{\kappa_{\beta\parallel}-1/2}{\kappa_{\beta\parallel}} + \left(\zeta_{\beta}^0-\zeta_{\beta}^s\right)\frac{\kappa_{\beta\perp}-2}{\kappa_{\beta\perp}}Z_{\kappa_{\beta\parallel}}^{(0)}(\zeta_{\beta}^s)+\frac{u_{\beta\perp}^2}{u_{\beta\parallel}^2}\zeta_{\beta}^s Z_{\kappa_{\beta\parallel}}^{(1)}(\zeta_{\beta}^s)\right], \tag{6}$$

where

$$\zeta_{\beta}^n = \frac{z-nr_{\beta}}{q_{\parallel}u_{\beta\parallel}}, \quad \zeta_{\beta}^0 = \frac{z}{q_{\parallel}u_{\beta\parallel}},$$

and where we have introduced dimensionless variables

$$z = \frac{\omega}{\Omega_*}, \quad q_{\parallel} = \frac{k_{\parallel}v_*}{\Omega_*}, \quad q_{\perp} = \frac{k_{\perp}v_*}{\Omega_*}, \quad r_{\beta} = \frac{\Omega_{\beta}}{\Omega_*},$$

with Ω_* and v_* being some characteristic angular frequency and velocity, respectively. For the present application, we make the convenient choice $v_* = v_A$, the Alfvén velocity, and $\Omega_* = \Omega_i$, the angular ion-cyclotron frequency. We have also introduced in Eq. (6) the plasma dispersion function of order m, defined for distributions with a κ parameter

$$Z_{\kappa}^{(m)}(\xi) = \frac{1}{\pi^{1/2}}\frac{\Gamma(\kappa)}{\kappa^{1/2}\Gamma(\kappa-1/2)} \times \int_{-\infty}^{\infty}\frac{ds}{(s-\xi)(1+s^2/\kappa)^{\kappa+m}}. \tag{7}$$

This plasma dispersion function can be written in terms of the Gauss hypergeometric function ${}_2F_1(a, b, c; z)$, as follows:

$$Z_\kappa^{(m)}(\xi) = \frac{i\Gamma(\kappa)\Gamma(\kappa+m+1/2)}{\kappa^{1/2}\Gamma(\kappa-1/2)\Gamma(\kappa+m+1)} \times {}_2F_1\left[1, 2\kappa+2m, \kappa+m+1; \frac{1}{2}\left(1+\frac{i\xi}{\kappa^{1/2}}\right)\right], \tag{8}$$

for $\kappa > -m - 1/2$. For $m = 1$, the plasma dispersion function given by Equations (7) and (8) is the same as the dispersion function defined by Summers and Thorne.[9,10]

Let us also consider the case of plasma particles which are described by bi-Maxwellian distribution functions

$$f_{\beta,M}(v_\parallel, v_\perp) = \frac{n_{\beta 0}}{\pi^{3/2} v_{\beta\perp}^2 v_{\beta\parallel}} \exp\left(-\frac{v_\parallel^2}{v_{\beta\parallel}^2} - \frac{v_\perp^2}{v_{\beta\perp}^2}\right), \tag{9}$$

where

$$v_{\beta\parallel}^2 = \frac{2T_{\beta\parallel}}{m_\beta}, \quad v_{\beta\perp}^2 = \frac{2T_{\beta\perp}}{m_\beta}.$$

Using the distribution function given by (9), we obtain

$$J(s,1,0;f_{\beta 0}) = 2n_{\beta 0}\left[-1 + \frac{u_{\beta\perp}^2}{u_{\beta\parallel}^2} + \left(\zeta_\beta^0 - \zeta_\beta^s + \frac{u_{\beta\perp}^2}{u_{\beta\parallel}^2}\zeta_\beta^s\right) Z\left(\zeta_\beta^s\right)\right], \tag{10}$$

where $Z(\zeta)$ is the well-known plasma dispersion function.[24]

Finally, we consider the case of plasma particles with BK velocity distributions

$$f_{\beta,\kappa}(v_\parallel, v_\perp) = \frac{1}{\pi^{3/2}\kappa_\beta^{3/2} v_{\beta\perp}^2 v_{\beta\parallel}} \frac{\Gamma(\kappa_\beta)}{\Gamma(\kappa_\beta - 3/2)} \times \left(1 + \frac{v_\parallel^2}{\kappa_\beta v_{\beta\parallel}^2} + \frac{v_\perp^2}{\kappa_\beta v_{\beta\perp}^2}\right)^{-\kappa_\beta}, \quad \left(\kappa_\beta > \frac{3}{2}\right). \tag{11}$$

For particles with a velocity distribution function as defined by Equation (11), the $J(s, 1, 0; f_{\beta 0})$ which appear in the dispersion relation for parallel propagating low frequency electromagnetic waves becomes as follows:

$$J(s,1,0;f_{\beta 0}) = 2n_{\beta 0}\left[-1 + \frac{u_{\beta\perp}^2}{u_{\beta\parallel}^2} + \left(\zeta_\beta^0 - \zeta_\beta^s + \frac{u_{\beta\perp}^2}{u_{\beta\parallel}^2}\zeta_\beta^s\right) \times \frac{\kappa_\beta - 3/2}{\kappa_\beta - 1} Z_{\beta\kappa}^{(-1)}\left(\zeta_\beta^s\right)\right]. \tag{12}$$

If different species are described by different forms or the distribution function, either PBK (Equation (3)), bi-Maxwellian (9), or BK (Equation (11)), the dispersion relation has to be written using in Equation (1) a proper combination of forms of the J integrals, (6), (10), or (12), respectively.

III. NUMERICAL ANALYSIS

For the numerical analysis, we have considered ion mass equal to proton mass and therefore ion charge number $Z_i = 1.0$, and we have considered the electron temperature as equal to the ion parallel temperature, $T_e = T_{i\parallel}$. For most of the cases shown, we have considered $v_A/c \simeq 1.0 \times 10^{-4}$ and $\beta_i \simeq 2.0$, as in well-known studies on space plasmas instabilities,[6] where $v_A = B_0/\sqrt{4\pi n_i m_i}$ is the Alfvén velocity, and $\beta_i = v_{i\parallel}^2/v_A^2$. However, we have also added one figure which shows results obtained considering the case of $\beta_i = 1.0$, in order to illustrate the effect of the change of the β parameter.

We have solved the dispersion relation considering different forms of the distribution functions for electrons and ions. In the figures, we show the imaginary part of the normalized frequency for waves in the ion-cyclotron branch, concentrating the analysis on the effect of the anisotropy due to the effective temperature of the ions on the growth rate of the ion-cyclotron instability.

In Figure 1, we show the imaginary part of the normalized wave frequency (z_i) vs. normalized wave-number, $q = kv_A/\Omega_i$, obtained from the solution of the dispersion relation, considering isotropic Maxwellian distribution for electrons and different forms of the ion distribution function. The column to the left shows the values of the growth rate γ, the positive values of z_i, while the right column shows the complete range of values of z_i. Figure 1(a) shows the results obtained for the case in which the ions are described by an anisotropic Maxwellian distribution, with $T_{i\perp}/T_{i\parallel} = 1.0$, 2.0, 3.0, 4.0, 5.0, 6.0, and 7.0. It is seen that instability occurs for values of temperature ratio above 1.0. The range of values of q which are unstable increases with the temperature ratio, as well as the magnitude of the growth rate at each value of q, and as well as the peak value of the growth rate. For $T_{i\perp}/T_{i\parallel} = 2.0$, which is the smaller value of the temperature ratio above 1.0 with results shown in the figure, the instability starts to be significant at $q \simeq 0.2$ and continues until $q \simeq 0.7$. For larger values of $T_{i\perp}/T_{i\parallel}$, the unstable range increases and the magnitude of the growth rate increases as well, so that for $T_{i\perp} = 7.0T_{i\parallel}$ the instability occurs between $q \simeq 0.1$ and $q \simeq 2.2$, with a maximum growth rate, which is slightly above ten times the maximum attained for temperature ratio 2.0. The situation depicted in Figure 1(a) corresponds to the conventional ion-cyclotron instability.

Figure 1(b) considers the case in which the ions are described by a PBK distribution, with $\kappa_{i\parallel} = \kappa_{i\perp} = 20$, and the same values of $T_{i\perp}/T_{i\parallel}$ considered in the case of Figure 1(a), with $T_e = T_{i\parallel}$. The curves representing γ and z_i, which are shown in Figure 1(b), are very similar in shape to those appearing in Figure 1(a). We only mention here that the values of z_i at the peak of the instability are slightly above those obtained in Figure 1(a), and that the unstable range is also slightly larger. For instance, for temperature ratio 7.0, the upper limit of the unstable range, which is $q \simeq 2.2$ in the case panel (a), is $q \simeq 2.4$ in the case of panel (b). The similarity between the results in (a) and (b) is not surprising, since the PBK distribution with $\kappa_{i\parallel} = \kappa_{i\perp} = 20$, considered in the case of panel (b), is not very different from a Maxwellian distribution.

In Figure 1(c), we depict the results obtained considering the ions described by a PBK distribution, with $\kappa_\parallel = \kappa_\perp = 5.0$ and $T_e = T_{i\parallel}$, and $T_{i\perp}/T_{i\parallel}$ ranging between 1.0 and 7.0, the same values of $T_{i\perp}/T_{i\parallel}$ used to obtain Figures 1(a) and 1(b).

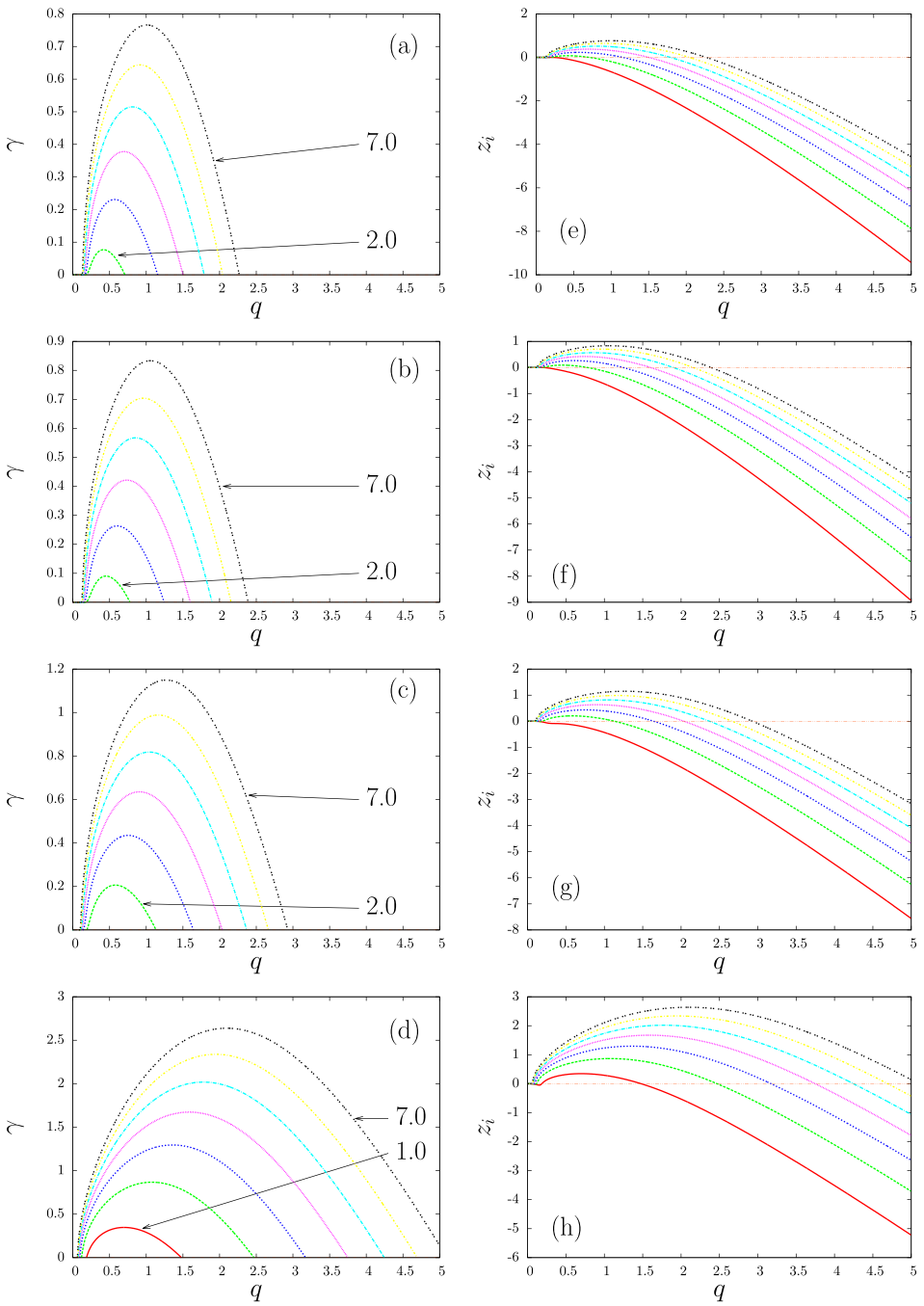

FIG. 1. Growth rate of instabilities (γ, left) and imaginary part of the normalized frequency (z_i, right), for waves in the ion-cyclotron branch vs. normalized wave number, considering isotropic Maxwellian distributions for electrons and different forms of the ion distribution function, and several values of the ratio $T_{i\perp}/T_{i\|}$. $\beta_i = 2.0$ and $v_A/c = 1.0 \times 10^{-4}$. (a) and (e) Ions with anisotropic Maxwellian distribution. (b) and (f) Ions with a PBK distribution with $\kappa_{i\perp} = \kappa_{i\|} = 20$. (c) and (g) Ions with a PBK distribution with $\kappa_{i\perp} = \kappa_{i\|} = 5.0$. (d) and (h) Ions with a PBK distribution with $\kappa_{i\perp} = \kappa_{i\|} = 2.5$. In all panels, the temperature ratios are $T_{i\perp}/T_{i\|} = 1.0$, 2.0, 3.0, 4.0, 5.0, 6.0, and 7.0.

The corresponding ratios of effective temperatures are $\theta_{i\perp}/\theta_{i\|} = 1.17$, 2.33, 3.50, 4.67, 5.83, 7.00, and 8.17. The ion distribution function is non-thermal and already quite different from a bi-Maxwellian with the same temperatures. Nevertheless, the results shown in Figure 1(c) are qualitatively similar to those appearing in Figures 1(a) and 1(b). The tendencies seen in the case of panel (b) continue to be observed in the case of panel (c). The values obtained for z_i in the case of panel (c) show that the instability is further increased by the non-thermal feature of the ion distribution function, as compared to the anisotropic Maxwellian case shown in Figure 1(a) and to the case with distribution closer to the anisotropic Maxwellian, as shown in Figure 1(b). The range of values of k, which are unstable, covers the region unstable in the bi-Maxwellian case, but the upper limit is extended toward larger values of q, and the lower limit also moves to $q \simeq 0.1$. The maximum growth rate, which is close to 0.8 in the case of Figure 1(a), is approaching 1.2 in the case of Figure 1(c).

In Figure 1(d), we depict the results obtained considering the ions described by a strongly non-thermal PBK distribution, with $\kappa_{\|} = \kappa_{\perp} = 2.5$ and $T_e = T_{i\|}$, and $T_{i\perp}/T_{i\|}$ ranging between 1.0 and 7.0, as in panels (a)–(c). The corresponding ratios of effective temperatures are $\theta_{i\perp}/\theta_{i\|} = 2.0$, 4.0, 6.0, 8.0, 10.0, 12.0, and 14.0. The ion distribution function in this case is very different from a bi-Maxwellian with the same temperature. The values obtained for γ in the case of Figure 1(d) show that the instability is meaningfully increased by the non-thermal feature of the ion distribution function for most of the range of q values, when compared to the case of anisotropic Maxwellian shown in Figure 1(a). The range of values of q which are unstable is extended toward the region $q \to 0$, for the same temperature ratio, when compared to

Figure 1(a), and the upper limit is very much increased and goes beyond $q = 5.0$. For instance, for temperature anisotropy $T_{i\perp}/T_{i\parallel} = 3.0$, which corresponds to ratio of effective temperatures equal to 6.0, the maximum growth rate is about 1.3, while for $T_{i\perp}/T_{i\parallel} = 6.0$ in the bi-Maxwellian case, Figure 1(a), the maximum growth rate is smaller, near the value 0.63. For $T_{i\perp}/T_{i\parallel} = 3.0$, Figure 1(a) shows that the maximum growth rate is even smaller, of course, only about 0.38.

It is also interesting to notice that in the case of Figure 1(d), the instability occurs even in the case of $T_{i\perp}/T_{i\parallel} = 1.0$, which corresponds to ratio of effective temperatures equal to 2.0. The presence of the instability for isotropic temperature parameters was not seen clearly in the case of slightly higher κ indexes, as in the case of $\kappa_{i\perp} = \kappa_{i\parallel} = 5.0$, in Figure 1(c).

The values of the real part of the normalized wave frequency, z_r, corresponding to the values of z_i shown in Figure 1, are depicted in Figure 2. The panels (a)–(d) of Figure 2 show the values of z_r corresponding, respectively, to panels (a)–(d) of Figure 1.

Figure 3 analyzes the effect of the form of the electron distribution function, by showing the values of γ for waves in the ion-cyclotron branch, obtained by considering a PBK distribution for the ions and two different forms of the electron distribution function. In Figure 3(a), it is depicted the case in which the electrons are characterized by an isotropic Maxwellian and the ions are characterized by a PBK distribution with $\kappa_{i\parallel} = \kappa_{i\perp} = 3.0$, with $T_{i\perp}/T_{i\parallel}$ ranging between 1.0 and 7.0. The situation is similar to that depicted in Figure 1(d), with the difference being the values of the κ indexes. The corresponding ratios of effective temperatures are $\theta_{i\perp}/\theta_{i\parallel} = 1.5$, 3.0, 4.5, 6.0, 7.5, 9.0, and 10.5. In Figure 3(b), we consider a case in which the ion distribution is equal to that considered for Figure 3(a), but the electron distribution is also a PBK distribution instead of a Maxwellian. We consider for Figure 3(b) the case of $\kappa_{e\parallel} = \kappa_{e\perp} = 3.0$, with isotropic temperatures, $T_{e\perp} = T_{e\parallel}$. The electron distribution is then highly non-thermal, with extended "tails" along parallel and perpendicular directions. It is seen that the consequence of the modification in the electron distribution function is a meaningful decrease in the growth rate of the instability. For instance, the comparison between panels (b) and (a) of Figure 3 shows that, for $T_{i\perp} = T_{i\parallel} = 7.0$, the maximum growth rate has decreased from a value close to 1.8 to a value near 1.4, only due to the change of the electron distribution function, from an isotropic Maxwellian to a PBK distribution with kappa indexes equal to 3.0, and isotropic temperatures.

In Figure 3, it is also noticed a sizable decrease of the unstable interval of wave-numbers. For example, in the case of temperature ratio equal to 7.0, the upper limit of the unstable range is near $q = 4.0$ for the case of electrons described by a Maxwellian distribution, in panel (a), and near $q = 2.8$ for the case of electrons described by a PBK distribution with kappa indexes equal to 3.0, in panel (b). The inference is that, despite the fact that the instability is generated by the anisotropy in the ion distribution, the increase in the non-thermal feature of the electron distribution affects the instability, as well, in this case reducing the growth rate. A similar influence of the electron distribution has already been reported in the case of the ion firehose instability.[21]

Figure 4 is dedicated to discuss on the differences between the influences of the anisotropy due to the ratio of temperatures and of the anisotropy due to the difference in the kappa indexes. Figures 4(a) and 4(b) show the values of γ obtained considering isotropic Maxwellian distribution for electrons and PBK distributions for ions, with $\kappa_{i\perp} = \kappa_{i\parallel}$, for the values 2.5, 5.0, 10.0, 15.0, 20.0, and 25.0. Figure 4(a) shows the case of $T_{i\perp}/T_{i\parallel} = 4.7$, while Figure 4(b) shows the case of $T_{i\perp}/T_{i\parallel} = 2.82$. The comparison between these two cases shows that, for a given value of the κ index, the unstable range of q tends to decrease with the decrease of the temperature anisotropy, and that the growth rates tend to

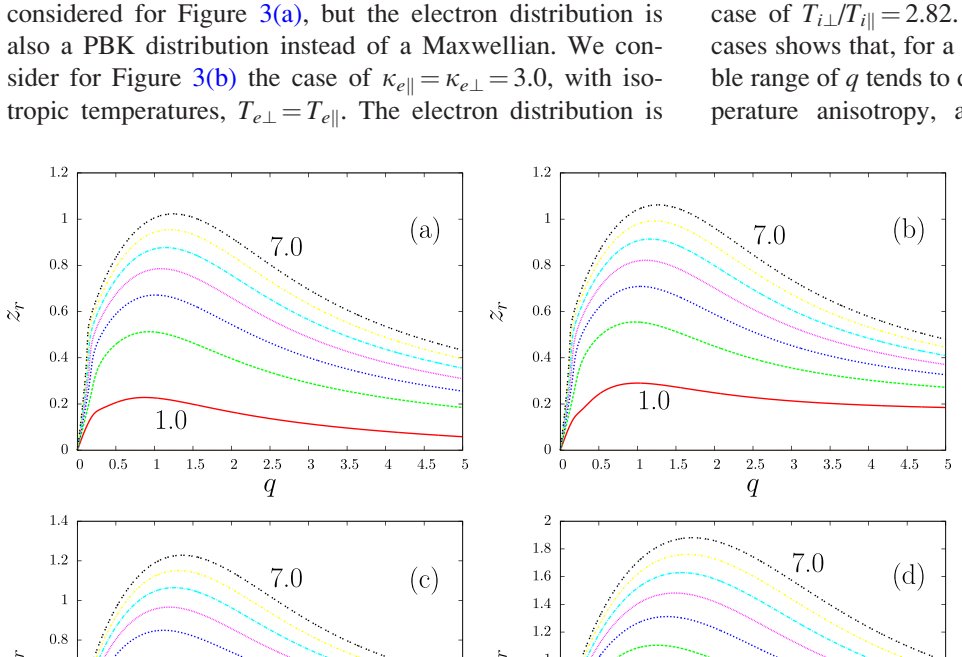

FIG. 2. Real part of the normalized frequency (z_r), for waves in the ion-cyclotron branch vs. normalized wave number, considering isotropic Maxwellian distributions for electrons and different forms of the ion distribution function, and several values of the ratio $T_{i\perp}/T_{i\parallel}$. The values of z_r which appear in this figure are the real counterparts to the values of z_i appearing in Figure 1. (a) Ions with an anisotropic Maxwellian distribution. (b) Ions with a PBK distribution with $\kappa_{i\perp} = \kappa_{i\parallel} = 20$. (c) Ions with a PBK distribution with $\kappa_{i\perp} = \kappa_{i\parallel} = 5.0$. (d) Ions with a PBK distribution with $\kappa_{i\perp} = \kappa_{i\parallel} = 2.5$. In all panels, the temperature ratios are $T_{i\perp}/T_{i\parallel} = 1.0$, 2.0, 3.0, 4.0, 5.0, 6.0, and 7.0.

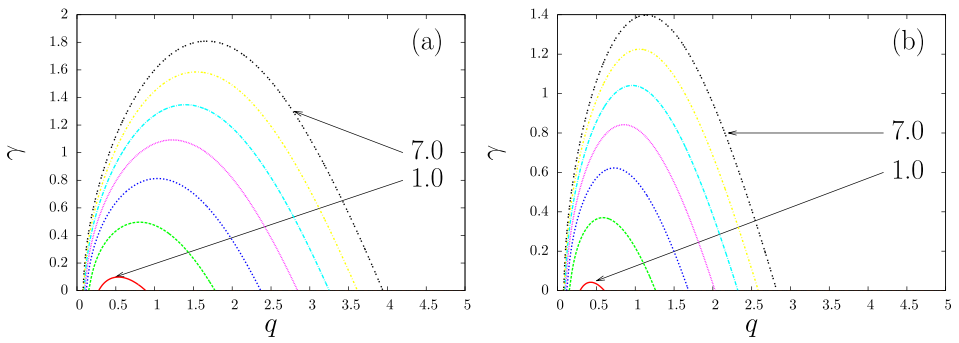

FIG. 3. Growth rate of instabilities (γ), for waves in the ion-cyclotron branch, vs. normalized wave number. (a) Electrons with an isotropic Maxwellian distribution, ions with a PBK distribution with $\kappa_{i\perp} = \kappa_{i\|} = 3.0$. (b) Electrons with a PBK distribution with $\kappa_{e\perp} = \kappa_{e\|} = 3.0$ and $T_{e\perp} = T_{e\|}$; ions with a PBK distribution with $\kappa_{i\perp} = \kappa_{i\|} = 3.0$. In both panels, the temperature ratios are $T_{i\perp}/T_{i\|} = 1.0$, 2.0, 3.0, 4.0, 5.0, 6.0, and 7.0.

decrease at each value of q. The two panels also show that, for a given value of the temperature ratio, the maximum growth rate decreases with the increase in the value of κ.

In Figure 4(c), we explore the anisotropy due to different values of $\kappa_{i\perp}$ and $\kappa_{i\|}$, by considering a case in which $T_{i\perp}/T_{i\|} = 1.0$, with $\kappa_{i\|} = 25.0$ and $\kappa_{i\perp} = 2.5$, 3.0, 5.0, 10.0, 15.0, 20.0, and 25.0, with isotropic Maxwellian for the electrons. The increase in $\kappa_{i\perp}$, for relatively large $\kappa_{i\|}$, corresponds to a decrease in perpendicular effective temperature, and therefore to a decrease of the anisotropy in the distribution function (the corresponding values of $\theta_{i\perp}/\theta_{i\|}$ are 4.7, 2.82, 1.57, 1.18, 1.08, 1.04, and 1.02). It is seen that only the cases with $\kappa_{i\perp} = 2.5$, 3.0, and 5.0 feature significant positive values of the growth rate. For $\kappa_{i\perp} > 5.0$, for which the ratio of effective temperatures is $\theta_{i\perp}/\theta_{i\|} \lesssim 1.5$, the instability does not occur.

In terms of the effective anisotropy, the red curve in Figure 4(c), obtained with $\kappa_{i\|} = 25$ and $\kappa_{i\perp} = 2.5$ ($\theta_{i\perp}/\theta_{i\|} = 4.7$), should be compared to the thin black curve in Figure 4(a), also obtained with $\kappa_{i\|} = 25.0$, but with $\kappa_{i\perp}$ also equal to 25.0, and anisotropy due to $T_{i\perp}/T_{i\|} = 4.7$. The two curves are practically identical, indicating that the amount of effective anisotropy is the driving factor for the ion-cyclotron instability, with small influence of the actual shape of the distribution.

In Figure 4(d), we investigate the effect of the electron distribution for a situation in which the anisotropy in the ion distribution is due to the κ indexes. We consider a situation where the ion distribution function is the same as in Figure 4(c), but the electron distribution is a PBK distribution, with $T_{e\perp} = T_{e\|}$ and $\kappa_{e\perp} = \kappa_{e\|} = 2.5$. The comparison between Figures 4(c) and 4(d) shows that also in this case the presence of non-thermal kappa-like features in the electron distribution contributes to decrease the instability, which is caused by the anisotropy in the ion distribution. The reduction occurs in the magnitude of the growth rate, for a given wave number, and also in the range of unstable wave numbers. The situation regarding the effect of the shape of the electron distribution, in a case where the anisotropy is due to anisotropic κ indexes in the ion distribution, as is the case shown in Figure 4, is similar to the situation depicted in Figures 3(a) and 3(b), in which the anisotropy was due to the difference between $T_{i\perp}$ and $T_{i\|}$.

In Figure 5, we analyze the effect of the parameter β_i, by considering situations which are similar to those considered for Figure 1, with the difference that we now use $\beta_i = 1.0$ instead of $\beta_i = 2.0$. The sequence of panels appearing in Figure 5 shows results which can be qualitatively described as those in Figure 1. However, the decrease in the factor β_i has caused some decrease in the magnitude of the growth rates, which is not very

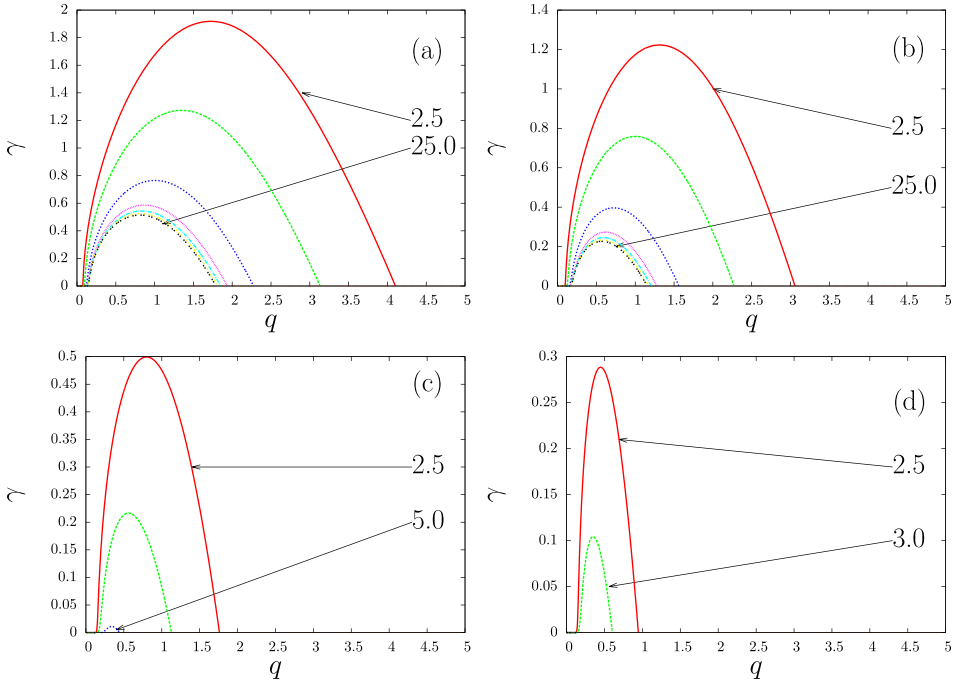

FIG. 4. Growth rate of instabilities (γ), for waves in the ion-cyclotron branch, vs. normalized wave number. (a) Isotropic Maxwellian distribution for electrons and PBK distribution for ions, with $T_{i\perp}/T_{i\|} = 4.7$ and several values of $\kappa_{i\perp} = \kappa_{i\|}$, 2.5, 3.0, 5.0, 10.0, 15.0, 20.0, and 25.0. (b) Isotropic Maxwellian distribution for electrons and PBK distribution for ions, with $T_{i\perp}/T_{i\|} = 2.82$ and several values of $\kappa_{i\perp} = \kappa_{i\|}$, 2.5, 3.0, 5.0, 10.0, 15.0, 20.0, and 25.0. (c) Isotropic Maxwellian distribution for electrons and PBK distribution for ions, with $T_{i\perp}/T_{i\|} = 1.0$, $\kappa_{i\|} = 2.5$, and several values of $\kappa_{i\perp}$, 2.5, 3.0, 5.0, 10.0, 15.0, 20.0, and 25.0 (values of $\theta_{i\perp}/\theta_{i\|}$ are 4.7, 2.82, 1.57, 1.18, 1.08, 1.04, and 1.02). (d) PBK distribution for electrons, with $T_{e\perp}/T_{e\|} = 1.0$ and $\kappa_{e\|} = \kappa_{e\perp} = 2.5$, and PBK for ions, with $T_{i\perp}/T_{i\|} = 1.0$, $\kappa_{i\|} = 2.5$, and several values of $\kappa_{i\perp}$, 2.5, 3.0, 5.0, 10.0, 15.0, 20.0, and 25.0.

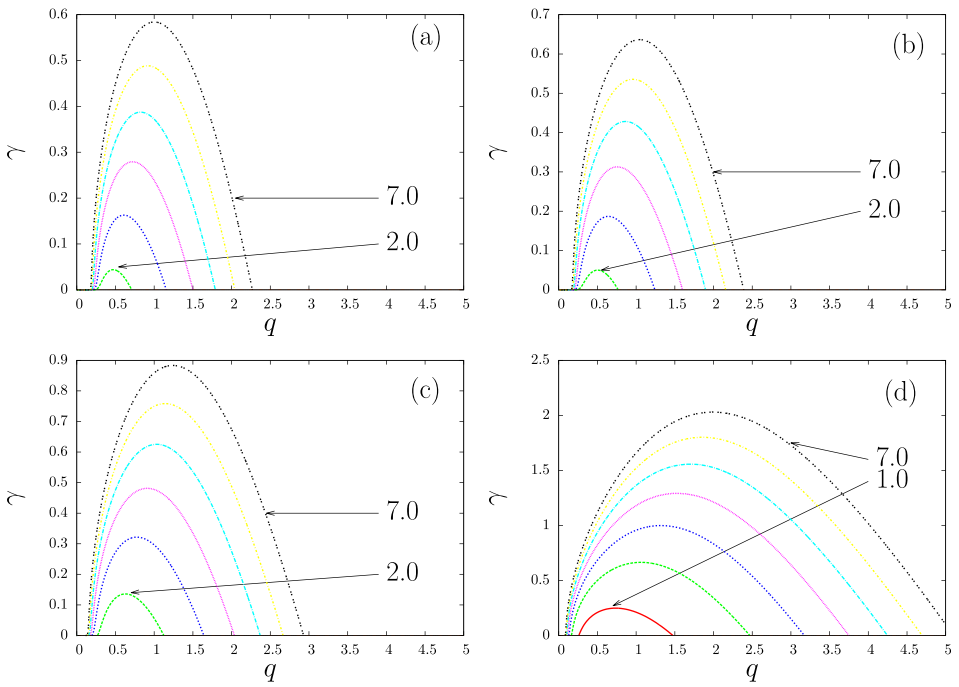

FIG. 5. Growth rate of instabilities (γ), for waves in the ion-cyclotron branch vs. normalized wave number, considering isotropic Maxwellian distributions for electrons and different forms of the ion distribution function, for several values of the temperature ratio, with $\beta_i = 1.0$ and $v_A/c = 1.0 \times 10^{-4}$. (a) Anisotropic Maxwellian distribution for ions. (b) Ions with a PBK distribution with $\kappa_{i\perp} = \kappa_{i\|} = 20$. (c) Ions with a PBK distribution with $\kappa_{i\perp} = \kappa_{i\|} = 5.0$. (d) Ions with a PBK distribution with $\kappa_{i\perp} = \kappa_{i\|} = 2.5$. In all panels, the temperature ratios are given by $T_{i\perp}/T_{i\|} = 1.0$, 2.0, 3.00, 4.0, 5.0, 6.0, and 7.0.

significant. For instance, for the case shown in panel (a) with $T_{i\perp}/T_{i\|} = 7.0$, the case of $\beta_i = 2.0$ features maximum value $\gamma \simeq 0.78$, while the case of $\beta_i = 1.0$ leads to maximum value of $\gamma \simeq 0.59$. Moreover, it is noticed that for the smaller value of β_i the magnitude of the effect associated with the non-thermal character of the distribution in approximately the same. For instance, the peak value of γ appearing in Figure 5(b) is about 0.63, while in Figure 5(a), it is nearly 0.59, a small difference. For the case of $\beta_i = 2$, Figures 1(b) and 1(a) show that the corresponding values are 0.83 and 0.78, also a small difference.

For distributions which are more distant from the Maxwellian case, as in panels (d) and (c) in Figure 5, the behavior is similar. It is seen that the value at the peak of γ in panel 5(d) is about 2.2 times the value at the peak in panel (c). In the case of Figure 1, the maximum values of γ in panels (d) and (c) feature a ratio near 2.3, very close to that of the case with smaller value of β_i, appearing in Figure 5. As already mentioned, the results obtained in the case of $\beta_i = 1.0$ are qualitatively similar to those obtained in the case of $\beta_i = 2.0$. These results, obtained for a relatively large range of β_i values, do not feature the same characteristics obtained in recent numerical analysis made considering a different form of PBK distribution.[17] A more detailed comparison between the dispersion relations associated with the two different forms of PBK distribution, for a large range of parameters, is clearly necessary. We intend to perform such a detailed analysis and report our findings in a forthcoming publication.

Finally, in Figure 6, we show some results that stress the effect of the form of the distribution functions and the effect of the increase in the non-thermal character of the distribution, on the ion-cyclotron instability. We consider $\beta_i = 2.0$, $v_A/c = 1.0 \times 10^{-4}$, and isotropic electrons with $T_e = T_{i\|}$. In the case of Figures 6(a) and 6(b), we consider electrons with isotropic Maxwellian distributions, and two forms of ion distribution function, for several values of $T_{i\perp}/T_{i\|}$. The thin lines are obtained with ions described by BK distributions, and the thick lines are obtained with ions described by PBK distributions. The difference between the panels (a) and (b) is that in the case of panel (a) the thin lines are obtained with $\kappa_i = 20.0$ and the thick lines are obtained with $\kappa_{i\perp} = \kappa_{i\|} = 20.0$, while in the case of panel (b), the thin lines are obtained with $\kappa_i = 5.0$, and the thick lines are obtained with $\kappa_{i\perp} = \kappa_{i\|} = 5.0$. The results depicted in Figure 6(a), case in which the ion distributions are not far from a Maxwellian distribution, show a small difference between the growth rates obtained in the case of ions with a BK distribution, compared with the case in which the ions have a PBK distribution, with the values obtained in the PBK case slightly larger than those obtained in the case of a BK distribution. On the other hand, the results obtained for small κ_i value, shown in Figure 6(b), show that the growth rate of the IC instability is considerably higher in the case of PBK distributions for ions, compared to the case of BK distributions with the same κ indexes. Not only is the growth rate larger, for a given wavelength, but also the range in wave number where the instability occurs is considerably larger in the case of PBK, than in the case of BK.

In Figures 6(c) and 6(d), we perform similar analysis, but considering that the electrons are described by an isotropic BK distribution, assuming $\kappa_e = \kappa_i$, for simplicity. By comparing Figures 6(c) and 6(a) and 6(d) and 6(b), it is seen that the change in the electron distribution, from Maxwellian to BK distribution, has negligible effect on the growth rate of the IC instability associated to ions with either BK or PBK distributions, both in the case of relatively large κ and in the case of small κ. Moreover, we also consider the case of electrons described by a PBK distribution, with isotropic kappa indexes, assuming $\kappa_{e\|,\perp} = \kappa_i$. By comparing the pairs of figures obtained in this case, Figure 6(e) for $\kappa = 20$ and Figure 6(f) for $\kappa = 5$, with Figures 6(a) and 6(c) and 6(b)

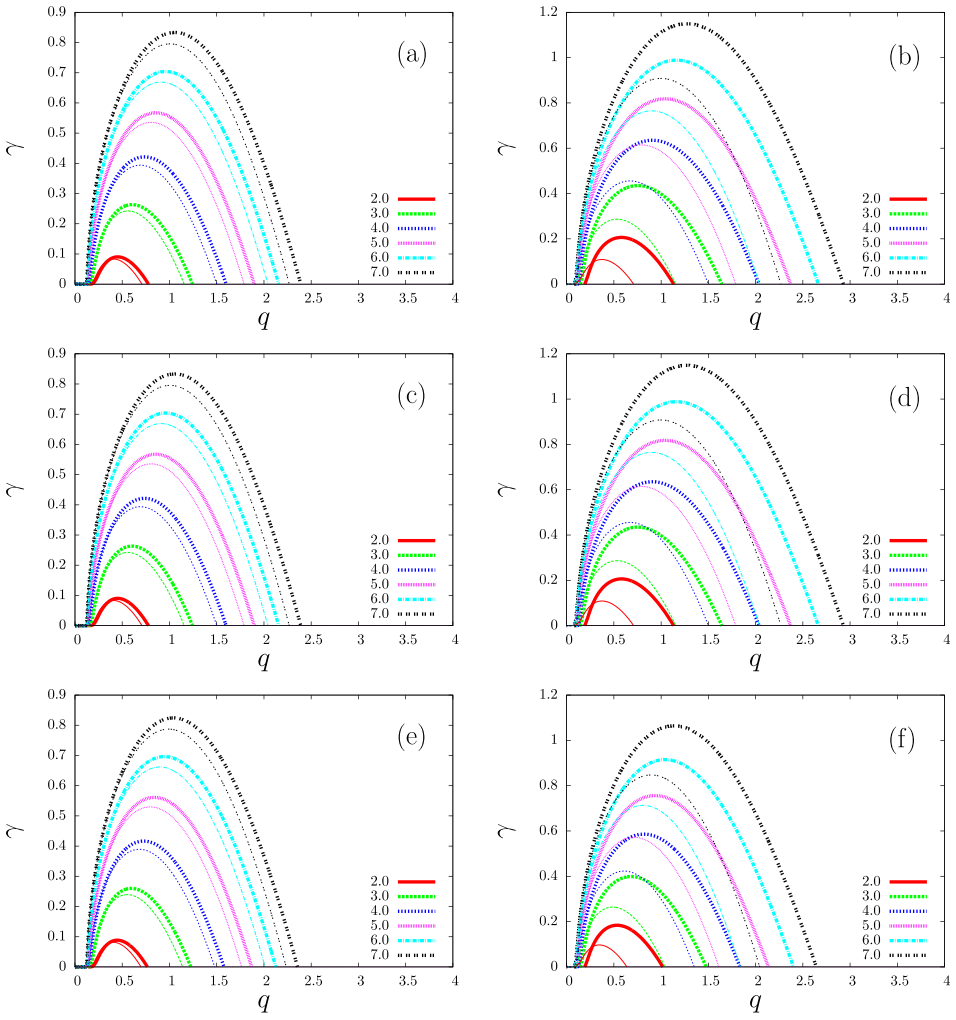

FIG. 6. Growth rate of instabilities (γ) for waves in the ion-cyclotron branch vs. normalized wave number, obtained by considering two different forms of the ion distribution function, for $\beta_i = 2.0$ and $v_A/c = 1.0 \times 10^{-4}$. (a) Thick lines: For ions, PBK distribution with $\kappa_{i\perp} = \kappa_{i\|} = 20$, and for electrons, isotropical Maxwellian; thin lines: For ions, BK distribution with $\kappa_i = 20$, and for electrons, isotropical Maxwellian. (b) Thick lines: For ions, PBK distribution with $\kappa_{i\perp} = \kappa_{i\|} = 5$, and for electrons isotropical Maxwellian; thin lines: For ions, BK distribution with $\kappa_i = 5$, and for electrons isotropical Maxwellian. (c) Thick lines: For ions, PBK distribution with $\kappa_{i\perp} = \kappa_{i\|} = 20$, and for electrons BK distribution with $\kappa_e = 20$; thin lines: For ions, BK distribution with $\kappa_i = 20$, and for electrons BK distribution with $\kappa_e = 20$; (d) thick lines: For ions, PBK distribution with $\kappa_{i\perp} = \kappa_{i\|} = 5$, and for electrons, BK distribution with $\kappa_e = 5$; thin lines: For ions, BK distribution with $\kappa_i = 5$, and for electrons, BK distribution with $\kappa_e = 5$; (e) thick lines: For ions, PBK distribution with $\kappa_{i\perp} = \kappa_{i\|} = 20$, and for electrons, PBK distribution with $\kappa_{e\perp} = \kappa_{e\|} = 20$; thin lines: For ions, BK distribution with $\kappa_i = 20$, and for electrons, PBK distribution with $\kappa_{e\perp} = \kappa_{e\|} = 20$; (f) thick lines: For ions, PBK distribution with $\kappa_{i\perp} = \kappa_{i\|} = 5$, and for electrons, PBK distribution with $\kappa_{e\perp} = \kappa_{e\|} = 5$; thin lines: For ions, BK distribution with $\kappa_i = 5$, and for electrons PBK distribution with $\kappa_{e\perp} = \kappa_{e\|} = 5$. For all panels shown, the temperature ratios are $T_{i\perp}/T_{i\|} = 1.0$, 2.0, 3.0, 4.0, 5.0, 6.0, and 7.0, and $T_e = T_{i\|}$.

and 6(d), respectively, we see that the modification of the electron distribution from a BK to a PBK leads to a small decrease in the magnitude of the instability and a small reduction in the range of unstable wave numbers, which can be easily perceived in the case of $\kappa = 5$ and is negligible in the case of $\kappa = 20$. These findings can be summarized in the statement that the change in the ion distribution, from a PBK distribution to a BK distribution, leads to a decrease in the magnitude and range of the growth rate of the IC instability, in all the three cases of electron distribution which have been considered, and that the effect is more pronounced for relatively small κ_i, that is, in the case of significant non-thermal tail in the ion distribution function. On the other hand, the modification of the electron distribution function, from a Maxwellian to a BK distribution, seems to have a negligible effect, while the adoption of PBK distribution for electrons leads to a decrease in the IC growth rate.

IV. REMARKS

We have presented and discussed some results originated from numerical solution of the dispersion relation for parallel propagating ion-cyclotron waves, considering that the velocity distribution of ions is a PBK distribution and concentrating the analysis in a parametric range where the ion-cyclotron instability occurs. We have also presented results obtained considering BK and bi-Maxwellian distributions, for comparison with the results obtained with PBK distributions. The effect of the shape of the electron distribution function has also been investigated.

The results which have been obtained in the numerical analysis show an enhancement of the ion-cyclotron instability due to the non-thermal features associated to the PBK distribution for ions, in comparison with results obtained when the ion distribution is an anisotropic Maxwellian distribution. It has

been shown that the range of values of wave number where the instability occurs covers the region unstable in the bi-Maxwellian case, but the upper limit is increased for decreasing κ indexes, that is, for increasing non-thermal feature of the ion distribution. The increase of the range of instability is particularly significant for small values of κ, such as $\kappa \leq 5.0$.

According to the numerical analysis which has been made, the qualitative effects associated to the non-thermal character of the PBK ion distribution are relatively independent of the plasma parameter β_i.

Concerning the effect of the electron distribution function on the growth rate of the ion-cyclotron instability, our results have shown that, for electrons described by PBK distributions, the increase in the non-thermal feature of the electron distribution affects in significant way the ion-cyclotron instability, leading to a reduction in the magnitude of the growth rate and to a reduction in the range of unstable wave-numbers. However, we have seen that, if the electrons are described by a distribution of type BK, the growth rate of the ion-cyclotron instability turns out to be nearly the same as that obtained in the case of Maxwellian distribution for electrons.

By comparing different forms of the ion distribution, we have verified that the change of the ion distribution from the BK distribution to a PBK distribution leads to an enhanced growth rate, regardless of the shape of the electron distribution, when considered the cases of Maxwellian, BK, and PBK distributions. The effect of the shape of the ion distribution function obtained in the case of IC instability is qualitatively opposed to the effect obtained from an investigation of the ion firehose instability.[21]

ACKNOWLEDGMENTS

R.G. acknowledges support from CNPq (Brazil), Grant Nos. 304461/2012-1 and 478728/2012-3. L.F.Z. acknowledges support from CNPq (Brazil), Grant No. 304363/2014-6. This work has also received partial support from Brazilian agency CAPES.

[1]W. Pilipp, H. Miggenrieder, M. Montgomery, K.-H. Mühlhäuser, H. Rosenbauer, and R. Schwenn, J. Geophys. Res. **92**, 1075, doi:10.1029/JA092iA02p01075 (1987).
[2]W. Pilipp, H. Miggenrieder, M. Montgomery, K.-H. Mühlhäuser, H. Rosenbauer, and R. Schwenn, J. Geophys. Res. **92**, 1093, doi:10.1029/JA092iA02p01093 (1987).
[3]J. C. Kasper, A. J. Lazarus, S. P. Gary, and A. Szabo, in *Proceedings of the 10th International Solar Wind Conference*, 2003, Vol. 679, p. 538.
[4]E. Marsch, X.-Z. Ao, and C.-Y. Tu, J. Geophys. Res. **109**, A04102, doi:10.1029/2003JA010330 (2004).
[5]E. Marsch, Living Rev. Sol. Phys. **3**, 1 (2006).
[6]S. P. Gary, *Theory of Space Plasma Microinstabilities*, Cambridge Atmospheric and Space Science Series (Cambridge, New York, 2005).
[7]S. P. Gary, H. Li, S. O'Rourke, and D. Winske, J. Geophys. Res. **103**, 14567, doi:10.1029/98JA01174 (1998).
[8]V. M. Vasyliunas, J. Geophys. Res. **73**, 2839, doi:10.1029/JA073i009p02839 (1968).
[9]D. Summers and R. M. Thorne, Phys. Fluids B **3**, 1835 (1991).
[10]R. L. Mace and M. A. Hellberg, Phys. Plasmas **2**, 2098 (1995).
[11]M. P. Leubner and N. Schupfer, J. Geophys. Res. **105**, 27387, doi:10.1029/1999JA000447 (2000).
[12]M. P. Leubner and N. Schupfer, J. Geophys. Res. **106**, 12993, doi:10.1029/2000JA000425 (2001).
[13]M. P. Leubner, Astrophys. Space Sci. **282**, 573 (2002).
[14]M. P. Leubner, Astrophys. J. **604**, 469 (2004).
[15]V. Pierrard and M. Lazar, Sol. Phys. **267**, 153 (2010).
[16]M. Lazar, Astron. Astrophys. **547**, A94 (2012).
[17]M. Lazar and S. Poedts, Mon. Not. R. Astron. Soc. **437**, 641 (2014).
[18]M. Lazar and S. Poedts, Astron. Astrophys. **494**, 311 (2009).
[19]M. Lazar and S. Poedts, Sol. Phys. **258**, 119 (2009).
[20]M. Lazar, S. Poedts, and R. Schlickeiser, Astron. Astrophys. **534**, A116 (2011).
[21]M. S. dos Santos, L. F. Ziebell, and R. Gaelzer, Phys. Plasmas **21**, 112102 (2014).
[22]M. Lazar, V. Pierrard, S. Poedts, and R. Schlickeiser, Astrophys. Space Sci. Proc. **33**, 97 (2012).
[23]R. A. Galvão, L. F. Ziebell, R. Gaelzer, and M. C. de Juli, Braz. J. Phys. **41**, 258 (2011).
[24]B. D. Fried and S. D. Conte, *The Plasma Dispersion Function* (Academic Press, New York, 1961).